Int. J. Electrochem. Sci., 12 **(2017)** 9212 – 9230, doi: 10.20964/2017.10.83

International Journal of
ELECTROCHEMICAL
SCIENCE
www.electrochemsci.org

Corrosion Inhibition of Low Carbon Steel in 1 M HCl Solution Using Pulicaria Undulata Plant Extract

A. S. Fouda[1,*], *M.Eissa*[2], *G. Y. Elewady*[1], *W.T. El behairy*[1]

[1] Chemistry Department, Faculty of Science, Mansoura University, El-Mansoura-35516, Egypt:
[2] Higher Institute of Engineering & Technology, Alex, Egypt and College of Science &Humanities-Harimlae, Shaqra University, KSA
[*]E-mail: asfouda@mans.edu.eg

Received: 16 June 2017 / *Accepted:* 22 August 2017 / *Published:* 12 September 2017

Pulicaria undulata (PU) plant extract was assessed as low cost, green and effective dissolution inhibitor for low C-steel (LCS) in 1 M HCl medium using mass reducing method, gasometric method, electrochemical impedance spectroscopy (EIS), Tafel polarization methods, EFM as well as surface studies by XPS, SEM and AFM techniques. Increasing PU extract concentration raises the R_{ct} and drops the C_{dl} as a result of the PU extract adsorption on the alloy surface. The polarization results showed the mixed-type inhibition behavior of the studied extract. The adsorption isotherm model of PU extract on steel surface followed Temkin adsorption isotherm in HCl solution. The inhibition mechanism of PU was explained according to the increasing the inhibition efficiency with temperature and the activation parameters which suggest significant chemisorption of the PU extract on the alloy surface. The XPS studies confirmed the formation of protective layer of PU extract on carbon steel surface. Results obtained used showed good agreement which confirm the potential use of PU extract as corrosion inhibitor for low carbon steel in acidic media

---

Keywords: PU, Adsorption, Corrosion inhibition, LCS, HCl, SEM, AFM, XPS

1. INTRODUCTION

A large amount of HCl is used in the chemical industries for removing of hazard traces and rust. Using of corrosion inhibitors successfully protects the metal against a corrosive medium. Several studies in this field using organic inhibitors have been published [1–5]. Generally, heterocyclic organic substances containing donating hetero atoms which showed pronounced inhibitory characteristics resulting from adsorption on the surface and blocking of the active areas with high efficacy. The biological toxicity of these compounds, especially organic phosphate, is documented specifically about their environmental harmful characteristics. From the standpoint of safety, the development of non-toxic and effective inhibitors is considered more important and desirable, nowadays, which are also called eco-friendly or green corrosion inhibitors [6-9]. These toxic effects have led to the use of natural products as anticorrosion agents which are eco-friendly and harmless. In recent days many alternative eco-friendly corrosion inhibitors have been studied and developed. Plant extracts are biodegradable, environmentally friendly inhibitors, renewable resources and low cost extraction [10]. The mainly extract components support the film foundation on the metal surface, hence reducing corrosion [11, 12]. Many plant extracts as corrosion inhibitors in acidic solutions were reported by many authors such as: *(Mahogany) Khaya senegalensis (LKS)* [13], brown onion peel [14], Cucumis sativus peel [15], Thevetia peruviana [16], Papaya Seed [17], Pimenta dioica leaf [18], *Pancratium Foetidum Pom [19]*, *Piper Nigrum L. Essential Oils Extracted* [20], *Nigella sativa* [21], *essential oil of seed Carum Carvi* [22]. The PU extract contain 8-epi-Ivalbin, 11β, 13-dihydro-4H-xanthalongin 4-O-β-D-glucopyranoside, 2α-Hydroxy-5αH-eudesma-4(15), Ivalin, Crispioside A, Crispioside B, Eupatolitin, 6-Methoxykaempferol, Patulitrin, Patuletin 3-O-β-D-glucopyranoside [23], 5α-hydroperoxyivalin, 8-epi-xanthanol, 2α-hydroxyalantolactone, xanthanol and isoxanthanol [24], The major constituents were carvotan acetone followed by δ-cadinene , α-cadinol , thujanol , epi-α-cadinene , carvacrol and 14-hydroxy α-muurolene [25].

This study test the PU extract role on the dissolution reaction of LCS in 1M HCl acid medium. The PU extract role is measured using gasometric method, mass loss method, polarization diagrams, EIS technique, SEM, AFM and XPS techniques.

2. EXPERIMENTAL TECHNIQUES

2.1. Materials and Solutions

Corrosion tests have been worked on specimens of low C-steel with the chemical composition: 0.046 % C, 0.900 % Mn, 0.007 % P, 0.002 % Si, and the remainder iron. The aggressive solution used was prepared by dilution of analytical reagent grade 34% HCl with bidistilled water. The stock solution (1000 ppm) of PU was used to prepare the desired concentrations by dilution with bidistilled water.

2.2.Methods

2.2.1.Gasometric method

The hydrogen evolution method is a useful technique that calculate the amount of hydrogen producing during a corrosion process .The used bottle must contact through a plastic tube to a burette .Initially, the air volume in the burette was measured .Finally, medium low carbon steel sheets were immersed in the test solution and the reaction bottle was enclosed. The amount of H_2 gas was measured by the decreasing of the aqueous solution level in the burette at fixed time intervals.

2.2.2. Mass loss method

Pre-weighed low carbon steel sheets were suspended in 100 ml of 1 M HCl without and with the different contents of PU extract ranging from 50 to 300 ppm .After different dipping time the samples were output, washed with bidistilled water, dried and weighted accurately.

2.2.3. Electrochemical Measurements

Electrochemical techniques were done using a typical three compartments glass cell consisting of the steel specimen as working electrode (1 cm^2), saturated calomel electrode (SCE) as a reference electrode, and a platinum wire as a counter electrode. All electrochemical measurements were performed using Gamry Instrument (PCI4/75 Potentiostat/Galvanostat/ZRA.

2.2.4 Scanning electron microscopy (SEM)

The surface morphology of the specimens was examined by SEM images were recorded using the instrument VEGA3 TESCAN model.

2.2.5 Atomic Force Microscopy (AFM)

The AFM images of polished, uninhibited and inhibited low carbon steel samples were carried out using Nano Surf Easy scan 2 Flex AFM instruments (Nano Technology center, Mansoura University).

3. RESULTS AND DISCUSSION

3.1. Hydrogen evolution method

The produced H_2 gas volume resulting from the corrosion reaction can be calculated. Results obtained by the hydrogen evolution method (in Fig.1) are matching with other methods including weight loss and electrochemical methods. The hydrogen volume is dependent on time of reaction according to eq (1):

$$V = K\,t \qquad \textbf{(1)}$$

Where, V is the H_2 gas volume ,time t and K is the corrosion rate. From the table (1), the extract decreases the H_2 gas volume and increases the protective percent [26]. The corrosion rate determines from eq.(2)

$$C.R = (Vt – Vi)/ t_t - t_i \qquad \textbf{(2)}$$

Vt and Vi are the volumes of hydrogen evolved at time t_t and t_i, respectively. Table (2) shows the corrosion reduced rate with rise of PU concentration. The protection efficacy was determined using Eq. (3)

$$\% \text{ IE} = [1- (V_{Ht} / V^0_{Ht})] \text{ x}100 \qquad \textbf{(3)}$$

Table 1. %IE and C.R of low C- Steel obtained from gasometric method after 120 min in 1 M hydrochloric acid for different PU extract concentrations at 30^{o}C

[Inh]. Ppm	Volume of hydrogen gas evolved, ml	C.R X10^{-3} ,ml/min	%IE
Blank	3.4	28.3	-
50	2.7	22.5	20.6
100	2.5	20.8	26.5
150	2.3	19.2	32.4
200	2.0	16.7	41.2
250	1.8	15.0	47.1
300	1.0	8.3	70.6

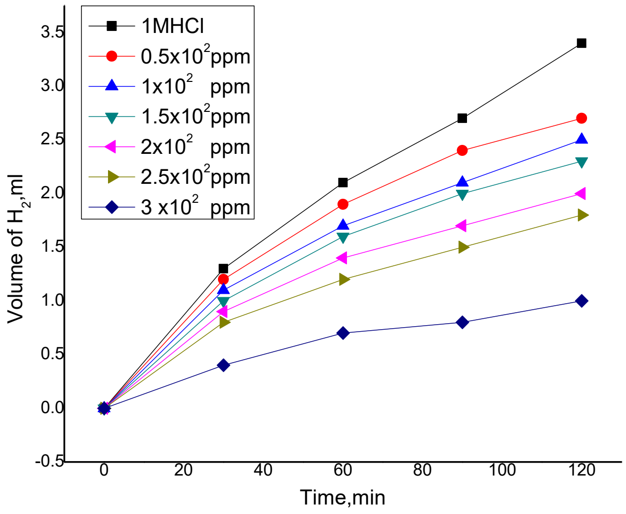

Figure 1. H_2 evolution from low C-steel dissolution in 1 M HCl in absence and presence of PU extract at 30^{o}C

3.2. Mass loss measurements

The losing in mass of low C- steel is measured, at different time periods, without and with of various extent of PU extract. The relationship between mass reduction and time are shows in Figure (2) for PU extract. The %IE affected by the contents of extract. The curves for different concentrations were fall below of the corrosive media. The rising in concentration of the extract give a decreasing of mass reduction and rise of the metal corrosion protection. Experimental data show that the PU extract is considers as inhibitory substance for low C- steel corrosion in 1M HCl medium. Also, the covered surface area (Θ) and inhibition efficiency due to the thin layer, founded by Eq. (4) [27], that rises with rise of the extract extent. The data recorded in table (2):

$$IE\ \% = \boldsymbol{\theta} \times 100 = [(W_o - W)/ W_o] \times 100 \qquad (4)$$

Where, W_o and W are the values of the uninhibited and inhibited weight loss, respectively".

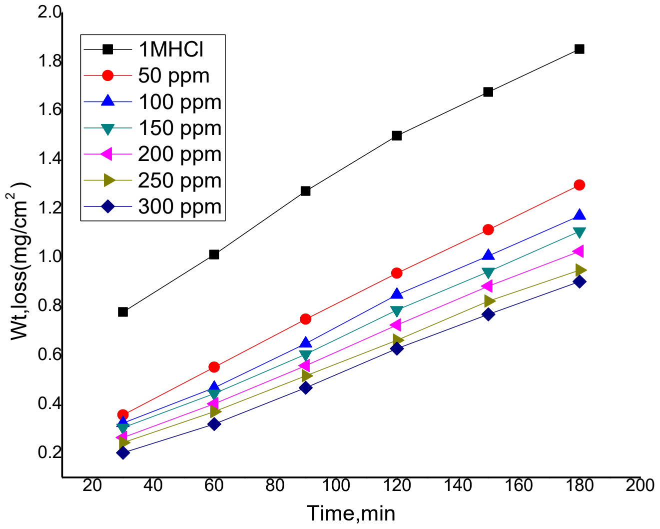

Figure 2. curves of mass losing vs time for the corroded low C-steel in 1M hydrochloric acid without and with the various PU concentrations at 30^o

Table 2. Percentage of protection and coverage of surface degree of PU extract for the low C- steel dissolution in hydrochloric acid from mass reduction data at various concentrations of PU extract at 30°C

[$_{inh.}$], ppm	Pulicaria extract	
	% IE	Θ
50	37.5	0.375
100	43.5	0.435
150	47.6	0.476
200	51.7	0.517
250	55.8	0.558
300	58.2	0.582

3.2.1. Adsorption isotherm

Temkin equation which is represented in Figures (3) used to calculate θ degree for PU extract. The covered surface area (θ) was calculated at several extract contents in 1 M hydrochloric acid media. The best fitting obeys the Temkin adsorption isotherm [28].

$$\Theta_{\text{coverage}} = (2.303/a) \text{ Log } C + (2.303/a) \text{ Log } K_{ads} \qquad (5)$$

K_{ads} is the adsorption constant, C is the concentration (mol L^{-1}) of the extract and "a" (Heterogeneous factor of surface of metal) .The values obtained of "a", K_{ads} and $\Delta G°_{ads}$ are presented in Table (3).

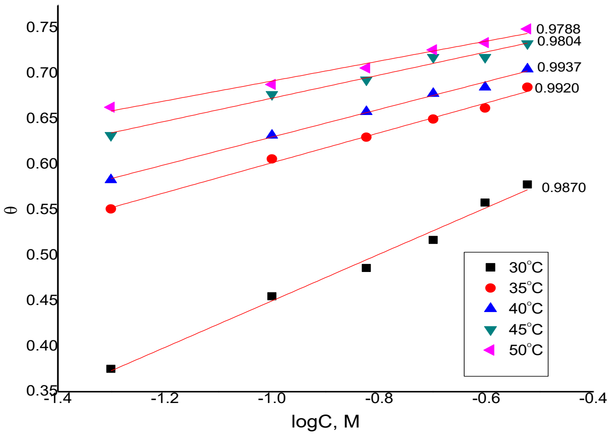

Figure 3. The diagram of Temkin adsorption of PU plant extract on the surface of low C- steel in 1 M HCl at different temperatures

Table 3.Some parameters from Temkin isotherm for LCS in 1M hydrochloric acid for PU plant extract at 30°C

Temp., K	$K_{ads}x10^{-5}$ M^{-1}	A	$-\Delta G^{\circ}_{ads}$ kJ mol^{-1}	ΔH°_{ads} kJ mol^{-1}	ΔS°_{ads} J mol^{-1} k^{-1}
303	0.01	8.9	26.1	412.1	1446
308	0.5	14.0	37.8		1461
313	1.3	15.1	41.3		1449
318	20.0	18.1	48.9		1450
323	199.5	21.0	56.0		1449

The K_{ads} is utilized to calculate the adsorption energy of ΔG^0_{ads} as follows:

$$K_{ads} = \frac{1}{55.5} \exp\left[\frac{-\Delta G^{\circ}_{ads}}{RT}\right] \qquad (6)$$

From Table (3), ΔG^o_{ads} depend on temperature. The value of ΔG^o_{ads} confirm the inhibitor adsorption is spontaneous and strength of the thin film on the metal which lead to rise of the disorder. From $\Delta G°_{ads}$ values, the adsorption of the PU components is physisorption. Positive values of (a) show the attractive forces between adsorbed molecules [29]. Large values of K_{ads} modify more effective adsorption and hence higher protective effective [30]. K_{ads} values are raise with rise in temperature indicate that the PU extract is chemically adsorbed. The high values of ΔH^o_{ads} indicate the chemisorption type [31].

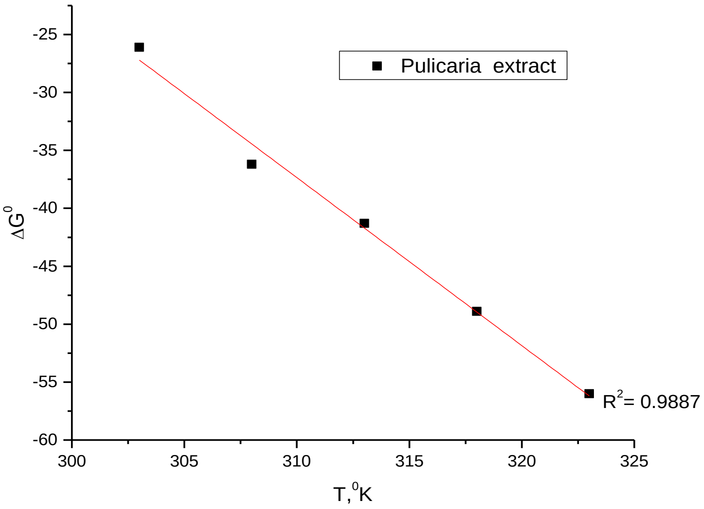

Figure 4. ΔG^o_{ads} vs T for the corrosion of low C-steel in the occurrence of PU extract

The random of adsorption can be measured from equation (7):

$$\Delta G^o_{ads} = \Delta H^o_{ads} - T\,\Delta S^o_{ads} \quad (7)$$

The calculated ΔH^o_{ads} and ΔS^o_{ads} were recorded in table (3). The calculated ΔH^o_{ads} value is positive which indicate that the endothermic adsorption process.

" The higher and positive values of ΔS^o_{ads} , indicating that the small molecules or ions such as H_2O , Cl^- interact with the surface atoms of low carbon steel are replaced by PU extract molecules that raises the disorder of the medium [32] "

3.2.2. Effect of temperature

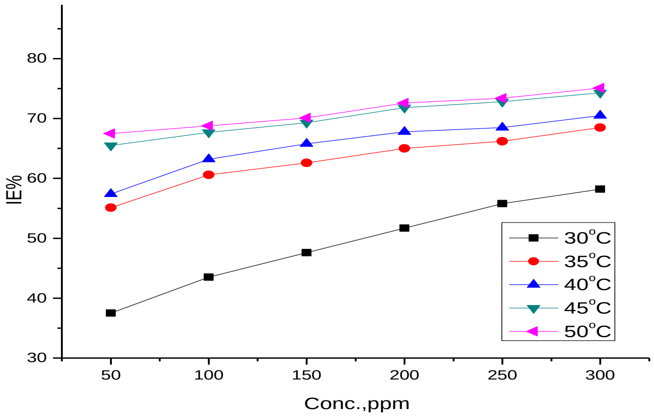

Figure 5. The role of concentration and temperature on the inhibition efficacy of PU extract;

Table 4. data efficiencies of inhibition , surface coverage degree (θ) and rate of the low C-steel dissolution in hydrochloric acid using mass reduction method with different PU extract concentrations at various temperatures.

Compound	Conc.,	Temp., C^o	C. R., mg cm$^-$	θ	% IE
Pulicaria extract	1M HCl	30	12	-	-
		35	22	-	-
		40	32	-	-
		45	37	-	-
		50	48	-	-
	50	30	7.8	0.375	37.5
		35	10.0	0.551	55.1
		40	13.5	0.574	57.4
		45	16.9	0.655	65.5
		50	17.3	0.675	67.5
	100	30	7.1	0.435	43.5
		35	8.8	0.606	60.6
		40	11.7	0.632	63.2
		45	15.9	0.677	67.7
		50	16.5	0.688	68.8
	150	30	6.5	0.476	47.6
		35	8.3	0.626	62.6
		40	10.9	0.658	65.8
		45	15.1	0.693	69.3
		50	15.9	0.701	70.1
	200	30	6.0	0.517	51.7
		35	7.8	0.650	65.0
		40	10.2	0.678	67.8
		45	13.9	0.718	71.8
		50	14.5	0.726	72.6
	250	30	5.5	0.558	55.8
		35	7.5	0.662	66.2
		40	10.0	0.685	68.5
		45	13.4	0.728	72.8
		50	14.1	0.734	73.4
	300	30	5.2	0.582	58.2
		35	7.0	0.685	68.5
		40	9.4	0.705	70.5
		45	12.6	0.743	74.3
		50	13.2	0.751	75.1

The corrosion rate of low C-steel in 1M HCl and with PU extract was tested in range of temperature from 303 to 323 K by mass reduction method (Fig.5). From table (4), both of the rate of corrosion and the percent of protection for PU extract were increases by rising of temperature. The increase of % IE with rising the temperature proves that at low temperatures the inhibitor adsorption is physisorption, but at high temperature is chemisorption [33-36].

3.2.3 Activation studies

The dissolution reaction parameters were measured from equation of Arrhenius (8):

$$\log k_{corr} = -E_a^*/2.303RT + \log A \qquad (8)$$

where *R* = universal gas constant, E_a= energy of activated complex, T = kelvin's temperature, and *A* = Arrhenius factor. From Table (5), the magnitude of E_a^* calculate from drawing of log k_{corr} against temperature reciprocal plots are shown in Figure (6). The E_a decreases in the PU occurrence due to delayed rate of adsorption with a resultant closer approach to equilibrium during the experiments at higher temperatures according to Hoar and Holliday[37]. But, Riggs and Hurd [38] explained that the reduction in the activation energy of corrosion at higher levels of inhibition arises from a shift of the net corrosion reaction from the uncovered part of the metal surface to the covered one". For the activated complex, the enthalpy change (ΔH^***)** and entropy change are calculated from Eq.(9):

$$k_{corr} = (RT/Nh)\exp(\Delta S^*/R)\exp(-\Delta H^*/RT) \qquad (9)$$

Where, k_{corr} is the metal corrosion rate, h is Planck's constant, N is Avogadro's number. Figure (6) indicate a draw of (log k/T) versus (1/T) with PU extract in hydrochloric acid (Table 5).

Table 5. Kinetic parameters for activated state of low C-steel without and with PU extract concentrations in 1 M hydrochloric acid

Conc ,ppm	Activation parameters		
	E^*a kJ mol^{-1}	ΔH^* kJ mol^{-1}	$-\Delta S^*$ J mol^{-1}K^{-1}
Blank	50.6	48.0	121.6
50	28.8	26.6	197.8
100	28.6	26.4	199.9
150	28.0	25.7	202.6
200	27.5	25.2	205.2
250	27.1	24.8	207.1
300	25.6	23.4	212.6

The activation energy decreases with rising of inhibitor content (Table 5), then the adsorption is chemical type. The positive ΔH^* indicates the extract adsorption is endothermic. The negative $\Delta S^*$with and without the extract shows that in the rate determining step, the association of unstable coordinated compound is more than the dissociation [39].

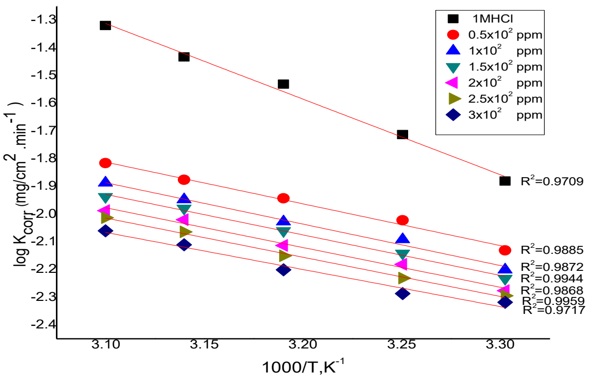

Figure 6. Diagram of Arrhenius (log K$_{corr}$ versus 1/ T) for dissolution of low C- Steel in 1 M HCl without and with different PU extract concentrations

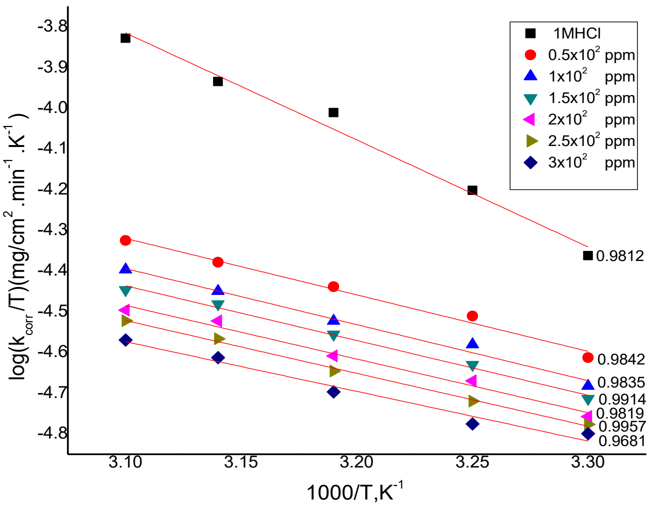

Figure 7. Diagram of (log k$_{corr}$ / T) versus 1/ T for dissolution of LCS in hydrochloric acid without and with different PU extract contents.

3.4. Electrochemical frequency modulation technique (EFM)

EFM is safely dissolution method that identified the current magnitude without meaningful of Tafel constants, and with only a small signal of polarizing [40]. Figure (8) shows the EFM spectrum of low C-steel in hydrochloric acid solution with various PU extract contents. From table (6) ,the addition of PU extract with different concentrations to the corrosive medium reduce the current density of corrosion, meaning that PU extract act as inhibitor by adsorption process. ”The causality factors are very closer to theoretical values which according to EFM theory [41] should prove the validity of Tafel slopes and corrosion current densities. %IE$_{EFM}$ raises by rising contents of extract and it can be measure using Eq.(10):

$$\%IE_{EFM} = [1-(i_{corr}/i^{o}_{corr})]\times 100 \qquad (10)$$

where i^{o}_{corr} and i_{corr} are corrosion current densities without and with of inhibitor, respectively.

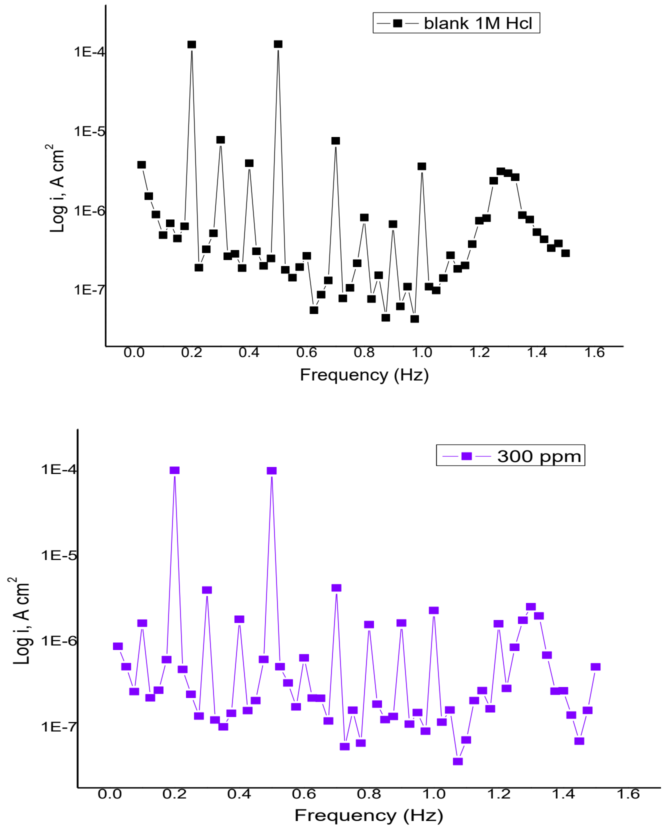

Figure 8. EFM spectrums for the dissolution of carbon steel in 1M HCl in absent and presence of 300 ppm of PU extract.

Table 6. EFM Parameters for low C-Steal in the absence and presence of many PU concentrations in 1M HCl at 25°C.

[inh],ppm	$i_{corr,}$ µAcm^{-2}	$\beta_{c,}$mVdec^{-1}	$\beta_{a,}$mVdec^{-1}	CF-2	CF-3	C.R, mpy	Θ	%IE
0.0	354.2	275.4	134.5	2.06	2.44	161.8	-	-
50	305.8	107.9	97.4	1.94	2.90	139.7	0.137	13.7
100	206.2	113.3	87.5	1.87	1.90	94.2	0.418	41.8
150	165.5	104.3	83.3	2.12	2.75	75.6	0.533	53.3
200	149.6	111.5	82.8	1.94	2.63	68.4	0.578	57.8
250	145.1	109.3	81.7	2.03	3.37	66.3	0.590	59.0
300	138.9	103.6	81.8	1.99	2.81	63.5	0.608	60.8

3.5. Electrochemical impedance spectroscopy (EIS) technique

Figure (9) indicate the resistance curves for low Carbon steel in 1M hydrochloric acid medium without and with PU extract. The Nyquist plots do not produce perfect semicircles due to the irregularity of frequency [42] resulting from the surface asymmetric and the roughness of the surface. The semicircular shape shows that the corrosion process is controlled by the charge transfer and the occurrence of PU does not change the mechanism of low C-steel dissolution [43].The addition of PU raises the Rct value in corrosive medium. The C_{dl} is reduces with rising of PU concentration. These results prove the occurrence of a protective adsorbed layer.

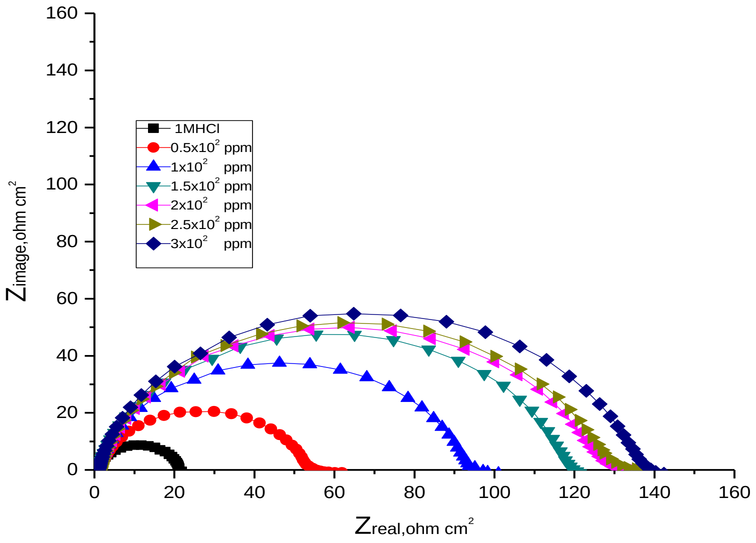

Figure 9. The Nyquist diagram for the low C-steel dissolution in hydrochloric acid without and with PU extract concentrations at 25°C

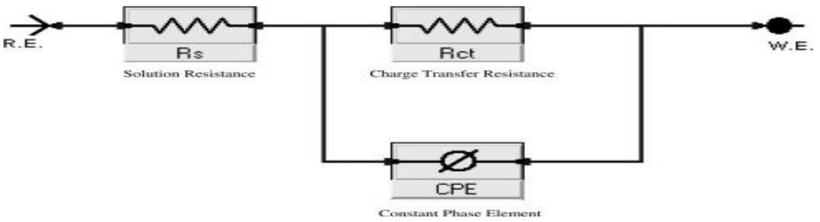

Figure 10. Equivalent circuit for fitting EIS data for low carbon steel in 1M hydrochloric acid solutions

From Fig. (10) the equivalent electrical circuit utilized for fitting the results. The C_{dl},Y_0 and n were measured by eq. (11) [44] :

$$C_{dl} = Y_0\omega^{n-1}/ \sin [n (\pi/2)] \qquad (11)$$

Where Y_0 is the CPE value, $\omega = 2\pi f_{max}$, f_{max} is the angular frequency, n is the exponential. From table 8, The CPE/C_{dl} decrease with a decreasing of dielectric factor and/or to an rising in the double layer thickness , advising that the extract components are adsorbed at the metal/solution interface[45] .The %IE can measured from equation (12) [46]:

$$\% IE_{EIS} = [1 -(R°_{ct}/ R_{ct})] \times 100 \qquad (12)$$

where R^o_{ct} and R_{ct} are the resistance of charge moving values in extract free and inhibitory solution respectively.

Table 7. Parameters measured by EIS method for low C-steel in 1M hydrochloric acid without and with PU extract concentrations at 25^{o}C

[inh.] ppm	R_S, Ωcm^2	Y^o, $\mu\Omega^{-1} s^n cm^{-2}$	N	R_{ct}, Ω cm^2	C_{dl}, μFcm^{-2}	θ	%IE
0.0	0.906	460.8	0.922	20.2	310.4	-	-
50	1.350	140.9	0.900	53.2	81.8	0.620	62.0
100	1.083	123.5	0.894	92.2	72.6	0.781	78.1
150	0.908	119.9	0.889	116.6	70.4	0.827	82.7
200	1.379	113.6	0.874	126.2	61.6	0.840	84.0
250	1.199	101.5	0.868	127.3	52.4	0.841	84.1
300	0.969	99.7	0.856	134.2	48.3	0.849	84.9

3.6. Potentiodynamic polarization curves

Figure (11) gives the polarization curves for low C-steel corrosion in one molar hydrochloric acid with and without PU extract extent at 25ºC. The protective percent and covered surface area are measured from eq. (13):

$$\%IE_p = [(i^o_{corr}–i_{corr}) / i^o_{corr}] \times 100 \quad = \theta \text{ x } 100 \qquad (13)$$

where i^o_{corr} and i_{corr} are the free and inhibited current densities, respectively. From table (8), the decrease of i_{corr} is clearly with increasing inhibitor concentration. The maximum displacement in E_{corr} is < 85 mV/E_{corr}, which consider that the PU is affected the reaction of both anodic and cathodic [47]. Additionally, this extract causes no change in the Tafel slopes, signifying that this extract is firstly adsorbed onto metal surface and therefore resist by only blocking the active positions with no change the reaction mechanism [48].

Table 9. dissolution voltage (E_{corr}), i_{corr}, Tafel constants (β_c,β_a), and covering surface area (θ), and protective percent (% IE_p) of low C- steel in hydrochloric acid at r.t for PU extract

[inh.] ppm	- E_{corr},mV (vs.SCE)	$i_{corr,}$ μA cm^{-2}	β_c mV dec^{-1}	β_a mV dec^{-1}	C.R, mpy	θ	% IE
0	522	375.0	114.0	96.3	171.3	---	---
50	517	256.0	110.8	91.8	117.1	0.317	31.7
100	514	160.0	104.9	87.6	73.2	0.573	57.3
150	506	119.0	107.2	88.5	54.2	0.683	68.3
200	507	107.0	107.2	82.2	48.7	0.715	71.5
250	503	97.2	104.0	79.7	44.4	0.741	74.1
300	503	77.6	106.6	83.0	35.5	0.793	79.3

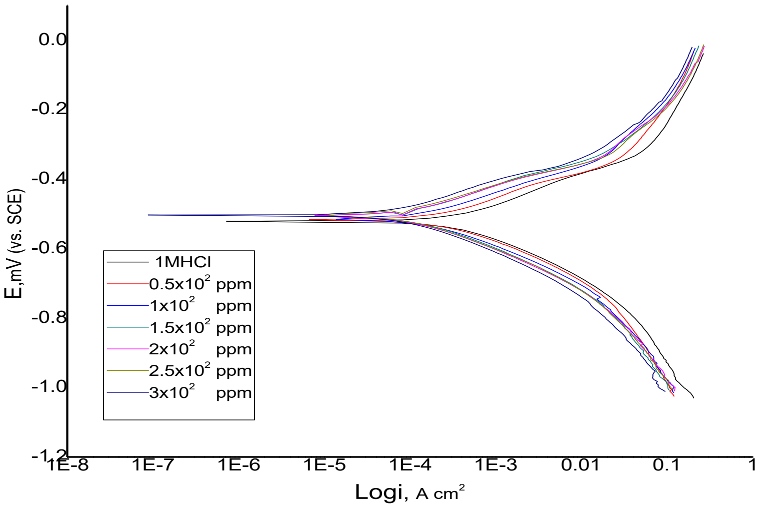

Figure 11. corrosion polarization plots for the low C-steel in 1M hydrochloric acid without and with PU extract concentrations at 25°C

3.7. Scanning electron microscopy (SEM) tests

Surface morphology of low carbon steel was evaluated by SEM after 24h dipping in 1M HCl before and after addition of inhibitor. The SEM micrograph of Figure 12(a) shows the smooth surface of low carbon steel. While Figure 12(b) shows that the surface with 1M HCl is very rough due to corrosion. However, the presence of 300 ppm PU, the surface coverage increases, proposing that the formation of a adsorbed inhibitory layer on the surface.

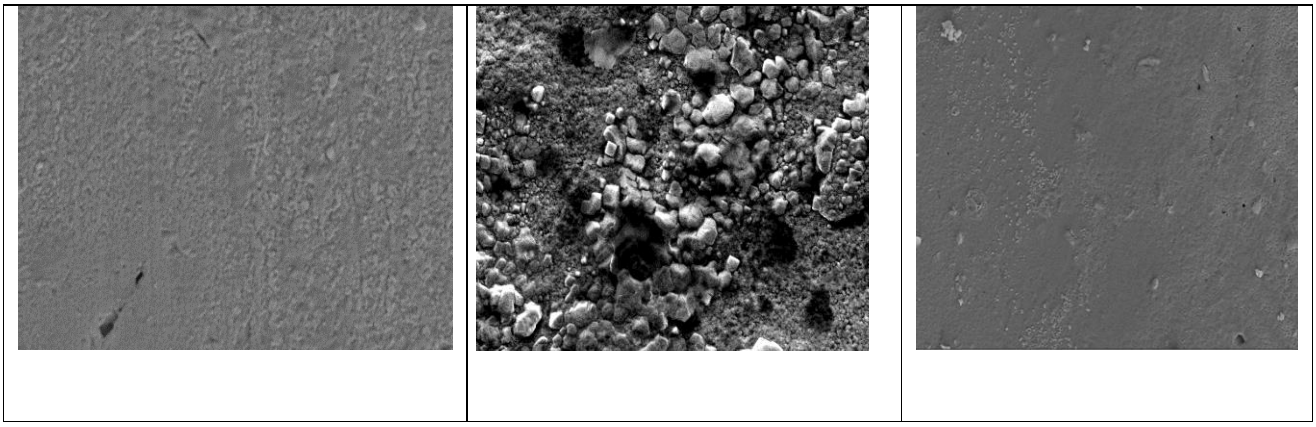

Figure 12. SEM micrographs of (a) polished low carbon steel (b) low carbon steel immersed in 1M HCl (c) low carbon steel immersed in1M HCl containing 300 ppm PU.

3.8. Atomic force microscopy (AFM) analysis

AFM provides images with atomic or near-atomic-resolution surface topography, capable of computing surface roughness of samples. The three dimensional (3D) AFM morphologies for polished low carbon steel surface and low C-steel surface in 1M HCl with and without PU extract are shown as Figure (13).

Table 10. AFM data for low C-steel surface dipped in inhibited and uninhibited medium.

Samples	The root mean square (nm)	Roughness Average (nm)	The peak-valley height (nm)
Polished low C-steel	18.1	14.1	99.1
low C-steel in 1M HCl	493.2	392.6	4699.8
Low C-steel in 1M HCl +300ppm PU	244.5	195.9	1569.4

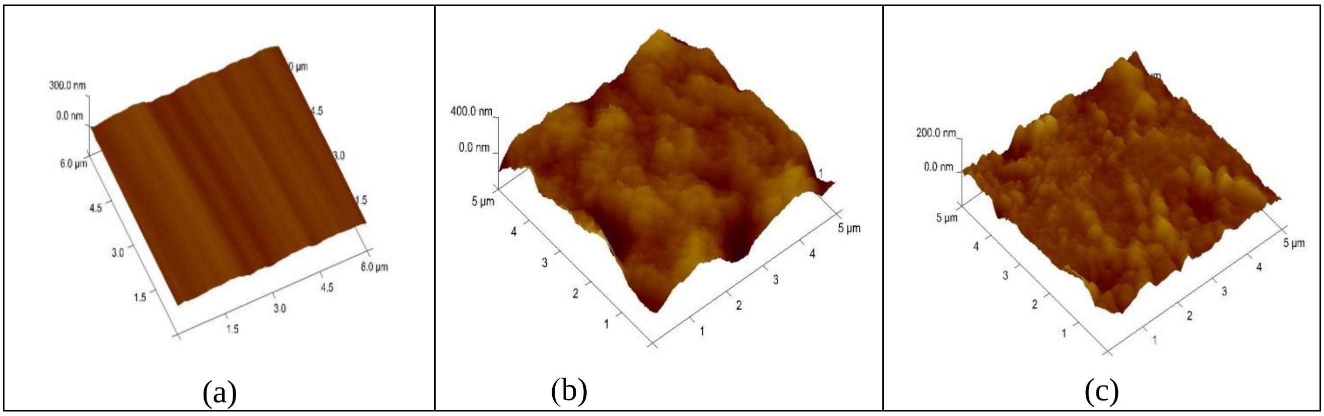

(a) (b) (c)

Figure 13. 3D AFM images of the surface of: a) As polished low carbon steel; b) low carbon steel immersed in 1M HCl; c) low carbon steel immersed in 1M HCl containing PU (300 ppm).

From Table 10 the metal surface in1M HCl has a greater surface roughness (392.6 nm) than the polished metal surface (14.1 nm), which shows that the sample is severely scratched due to the acid attack. The average roughness of protected steel is reduced and becomes (195.9 nm). The smoothness of the surface is due to the formation of a compacted adsorbed film on the surface thereby preventing the corrosion of steel [49].

3.9. X-Ray photoelectron spectroscopy (XPS) analysis

XPS technique gets deep insight about the chemical nature of the interface between the studied inhibitor and the steel surface. The XPS spectra of Fe 2p, O 1s, Cl 2p, and C 1s obtained for C-steel surface after dipping in 1 M hydrochloric acid solution in occurrence of 300ppm of PU extract for 24 hour following deconvolution by curve fitting were shown in Fig. 14. The Fe 2p spectrum showed two peaks located at a binding energy (BE) of 710.92 eV for Fe 2p3/2 and 725 eV for Fe 2p1/2 (14 a). The Fe 2p3/2 spectrum showed mainly five peaks. The Fe 2p3/2 spectrum showed a peak located at lower binding energy (710.92 eV) which is corresponding to metallic iron [50]. Also, the peak at (713.54 eV) is attributed to the presence of $FeCl_3$ on the metal surface [51] while the peak located at 720.00 eV is corresponding to the Fe^{3+} satellite [52]. Moreover, the peaks at 725 eV and 727.35 eV were attributed to Fe $2p_{1/2}$ due to the presence of α-Fe_2O_3, Fe_3O_4 and FeOOH [53]. The spectrum of O 1s (Fig. 14b) is deconvoluted into two peaks, the first one at 532.61 eV which assigned to C–O bond [54], whereas the second peak located at 533.83 eV binding energy which related to the C-O-C aromatic bonds [55]. The Cl 2p is deconvoluted into two peaks located at 198.9 eV for Cl 2p3/2 and 201.5 eV for Cl 2p1/2 (Fig. 14c) [56]. The C1s spectra could be deconvoluted into three components located at 284.8, 286.4, 288.6 eV (Fig. 12d). The largest peak at 284.8 can be attributed to the C-C bond of aromatic rings. Moreover, the peaks located at 286.4, 288.6 eV are attributed due to the COO and C=O bonds, respectively [57]. The peak located at 288.6 eV which assigned to C = O shows that PU extract molecules have been adsorbed on the surface [58]. Finally, the XPS spectrum proved that the inhibitive film formed on the surface consists of mixtures of compounds containing C and O atoms which prove the formation of inhibitive layer of the studied PU extract.

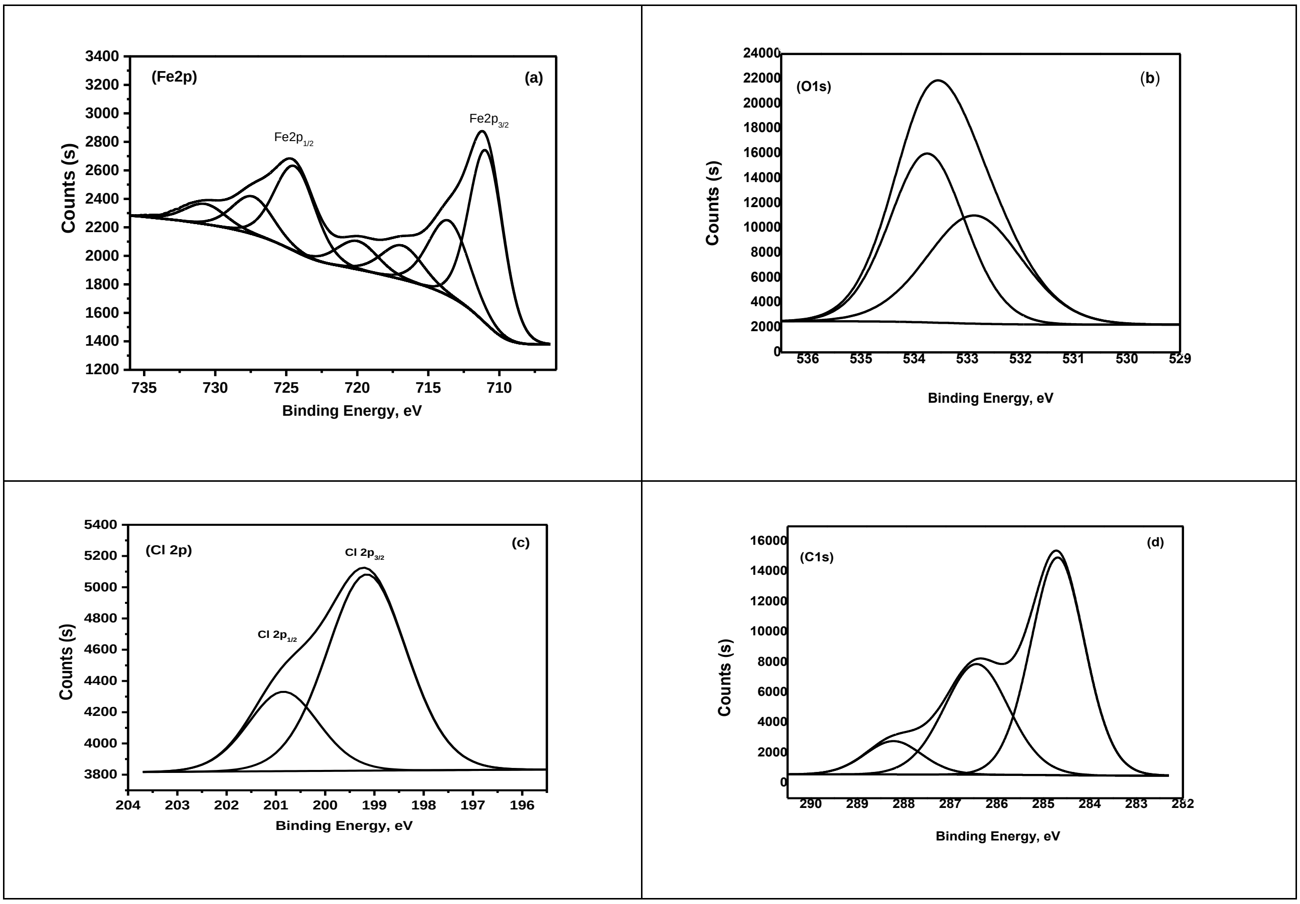

Figure 14. XPS deconvoluted profiles of (**a**) Fe 2p, (**b**) O 1s, (**c**) Cl 2p, and (**d**) C 1s, for low C-steel in 1 M HCl.

3.10. Mechanism of inhibition

According to electrochemical measurements, the addition of PU extract leads to retarding the low C-steel corrosion. From the results, the mechanism of inhibition involving blocking of surface active sites by adsorption of PU. The mechanism of PU adsorption involves a physisorption. Phytochemical analysis of PU extract indicate the existence of hetero atoms such as –N, –O, which strongly adsorption properties onto a low carbon steel surface. The inhibitory properties of these components may be recognized to their adsorption via the –NH, C=O, OH, *etc*. groups and also may be because of the presence of π- electrons in the rings. These organic molecules get adsorption on the metal surface making a protection layer and therefore the inhibition manner [59].

4. CONCLUSIONS

PU extract has good corrosion inhibitory on low C-steel in hydrochloric acid medium as confirmed by XPS results. Polarization plots data mention that the PU extract affected the reaction of both anodic and cathodic. %IE of PU extract rise with temperature rising but the activation energy of corrosion was decreased (chemisorption). The adsorption of PU extract obeys the Temkin equation. SEM and AFM techniques give information about morphology, topography and the roughness of the metal surface. There is good agreement between chemical and electrochemical techniques.

References

1. R.A. Prabhu, T.V. Venkatesha, A.V. Shanbhag, G.M. Kulkarni and R.G. Kalkhambkar, *Corros. Sci.*, 50 (2008)3356
2. N.E. Hamner, Corrosion Inhibitors, ed. C.C. Nathan, NACE Houston, Texas, USA, (1973)1
3. W.H. Li, Q. He, S. Zhang, C. Pei and B. Hou, *J. Appl. Electrochem.*, 38(2008) 289
4. S.A. Ali, H.A. Al-Muallem, S.U. Rahman and M.T. Saeed, *Corros. Sci.,*50 (2008)370
5. S.T. Arab and E.A. Noor, *Corros.*, 49(1993) 122
6. Z. Faska, A. Bellioua, M. Bouklah, L. Majidi, R. Fihi, A. Bouyanzer, B. Hammouti, Monatshefte für Chemie, 139 (2008) 1417.
7. O. C. Akalezi, K.C. Enenebaku, E.E. Oguzie, J. Mater. Environ. Sci., 4 (2013) 217.
8. M. Ramananda Singh, J. Mater. Environ. Sci., 4 (2013) 117.
9. O. Benali, H. Benmehdi, O. Hasnaoui, C. Selles, R. Salghi, J. Mater. Environ. Sci., 4 (2013) 127
10. A. Lecante, F. Robert, P.A. Blandinieres , C. Roos, *Curr. Appl. Phys.*,1 (2011) 714.
11. R.M.H. Lemmens , N. Wulijarni-Soetjipto, Plant Resources of South-East Asia, No. 3: Dye and Tannin-Producing Plants, Pudoc. Wageningen, (1991)
12. P. B. Raja , M. G. Sethuraman, *Mater. Lett*, 62(2008)113.
13. I.H. Ali, *Int. J. Electrochem. Sci.,* 11 (2016) 2130
14. K. C. R. Ferreira, R. F. B. Cordeiro, J. C. Nunes, H. Orofino, M. Magalhães, A. G. Torres, E. D'Elia, *Int. J. Electrochem. Sci.*, 11 (2016) 406
15. G.M. Al-Senani, *Int. J. Electrochem. Sci.*, 11 (2016) 291
16. A. S. Fouda, H. E. Megahed, N. Fouad, N. M. Elbahrawi, *J Bio Tribo Corros,* 2:16(2016) 1
17. S.Paul, I.Koley, *J Bio Tribo Corros,* 2:16 (2016) 2
18. K.K.Anupama, K. Ramya, K.M. Shainy, A.Joseph, Mater. Chem. Phys., 167(2015) 28
19. H. Bendaif, A. Melhaoui, M. El Azzouzi, B. Legssyer, T. Hamat, A. Elyoussfi, A. Aouniti, Y. El Ouadi, M. Aziz, *J. Mater. Environ. Sci.,*7 (4) (2016) 1276
20. R. Rmili, H. Elmsellem, M. Ramdani, B. El Mahi, Z. Ghazi, A. Chetouani, A. Aouniti, B. Hammouti, *J. Mater. Environ. Sci.,*7 (7) (2016) 2646

21. R. Souli, E. Triki1, P. Berçot, M. Rezrazi, B. Jaouad, A. Derja, L. Dhouibi,*J. Mater. Environ. Sci*., 6 (10) (2015) 2729
22. L. El Hattabia, M. EL Moudanea, H. Harharb, A. Bellaouchoua, A. Ghanimia, A. Guenboura, J. Costac, J. M. Desjobertc and M. Tabyaoui, *J. Mater. Environ. Sci.*, 7 (9) (2016) 3162
23. T.A. Hussien, S.A. El-Toumy, H.M. Hassan, M.H. Hetta, *Int J Pharm Pharm Sci*,8(9)(2016)150
24. M.Elamir, F. Hegazy, H.Matsuda, S.Nakamura, M.Yabe, T.Matsumoto , M.Yoshikawa, *Chem. Pharm. Bull.*, 60(3) (2012)363
25. M.Boumaraf, R.Mekkiou, S.Benyahia, J.C.Chalchat, P.Chalard, F.Benayache, S.Benayache, *Inter. J. of Pharmacognosy and Phytochemical Research*, 8(5) (2016)746
26. J.O.M. Bockris, D. Drazic, *Electrochim. Acta*,7(3) (1962) 293
27. El-Etre, A. Y. *Mater. Chem. Phys.*, 108 (2008) 278
28. A. N. Frumkin, Hydrogen overvoltage and adsorption phenomena. In: Delahay P, Tobias CW (eds) Advances in electrochemistry and electrochemical engineering, vol 3, chapter 5. Interscience Publisher Inc., New York, (1963)].
29. E.A. Noor, *Int. J. Electrochem. Sci.*,2 (2007) 996
30. S.A.M. Refray, F. Taha, A.M. Abd El-Malak, *Appl. Surf. Sci.*, 236 (2004)175
31. W. Durnie, R.D Marco, A. Jefferson, B. Kinsella, *J Electrochem. Soc.*, 146 (1999) 1751
32. L.Li , Q. Qu , W. Bai , F. Yang , Y. Chen , S. Zhang , Z. Ding, *Corr. Sci.*,59 (2012) 249
33. E.S Ivanov, Inhibitors for Metal Corrosion in Acid Media, Metallurgy, Moscow, 1986.
34. S.A. Umoren, I.B. Obot, E.E. Ebenso, P.C. Okafor, O. Ogbobe, E.E. Oguzie, *AntiCorros. Meth. Mater.*, 53 (2006) 277
35. A.Y. El-Etre, *Corros. Sci*.,45 (11) (2003) 2485
36. M. Abdallah, *Corros. Sci.*,46 (8) (2004) 1981
37. T.P Hour , R.D Holliday, *J. Appl Chem*, 3 (1953) 502
38. L.O Riggs (Jr) , T.J Hurd, *Corros.*,23(8) (1967) 252
39. S.S. Afak, B.Duran, A.Yurt, *Corros. Sci.*, 54 (2012)251
40. E.Kus, F.Mansfeld, *Corros., Sci.* 48(4) (2006) 965
41. A. Abdel Nazeer, N.K. Allam , A.S. Fouda, E.A. Ashour , *Mater. Chem. Phys.*, 136 (2012) 1
42. M.El Achouri, S.Kertit, H.M.Gouttaya, B.Nciri, Y.Bensouda, L.Perez, M.R.Infante, K.Elkacemi, *Prog. Org. Coat.*, 43(4) (2001) 267
43. K. Shalabi , A.Abdel Nazeer, Protection of Metals and Physical Chemistry of Surfaces, 51(5)(2015) 908
44. S. F.Mertens, C.Xhoffer, B. C.Decooman, E. Temmerman, *Corros.*,53 (5) (1997) 381
45. S. Ghareba, S. Omanovic, *Electrochim. Acta.*, 56(11) (2011) 3890
46. Ma H., Chen S., Niu L. Zhao S., Li S., Li D., *J. Appl. Electrochem.*, 32(1) (2002) 65
47. M. El Faydy, M. Galai, A. El Assyry, A. Tazouti, R. Touir, B. Lakhrissi, M. Ebn Touhami, A. Zarrouk, j. Mol. Liq. ,219 (2016) 396
48. K.F. Khaled*, *Electrochem. Acta*,53 (2008) 3484
49. P.N. Devi, J. Sathiyabama , S. Rajendran, *Int. J. Corros. Scale Inhib.*, 6(1) (2017)18
50. K. Boumhara, M. Tabyaoui, C. Jama, F. Bentiss, *J.Ind. and Eng. Chem.*,29 (2015)146
51. V.S. Sastri, M. Elboujdaini, J.R. Brown, J.R. Perumareddi, *Corrosion (Houston)*, 52 (1996) 447.
52. N. El Hamdani, R. Fdil, M. Tourabi , C. Jama , F. Bentiss ,Appl. Surf. Sci., 357 (2015)1294
53. X. Gao, S. Liu, H. Lu, F. Gao, H. Ma, Ind. Eng. Chem. Res.,54(2015)1941
54. J.L. Droulas, T. Minhduc, Y. Jugnet, *les Couches Minces*, 88 (1991) 39
55. C.A. Kovac, J.G. Clabes, M.J. Goldberg , *J. Vac. Sci. Technol.*, A 6 (1988) 991
56. T. Gu, et al., *Corros. Sci.*, 90 (2015)118
57. C. Maxime, R. Florent, A. Nadine, T. Michel, R. Christophe, L. Mounim, *Electrochim. Acta*, 131 (2014) 96
58. P. Mourya, P. Singh, A. K.Tewari, R. B. Rastogi ,M. M. Singh, *Corros.Sci.*, 95(2015)71

59. C.O. Akalezi, C.E. Ogukwe, E.A. Ejele and E.E. Oguzie, *Int. J. Corros. Scale Inhib.*,5(3) (2016)232